Journal of Molecular Structure 1313 (2024) 138667

Contents lists available at ScienceDirect

Journal of Molecular Structure

journal homepage: www.elsevier.com/locate/molstr

# Synthesis and biological activities of pyridine *N*-oxide bearing 5-aminoisoxazoles as potential acetylcholinesterase and monoamine oxidase inhibitors for Alzheimer's disease

Lange Yakubu Saleh [a,b,*], Soner Özdemir [b], Begüm Nurpelin Sağlık [c], H. Ali Döndaş [d,e], Cevher Altug [b]

[a] Department of Chemistry, University of Turku, Henrikinkatu 2, 20500 Turku, Finland
[b] Department of Chemistry, Bolu Abant Izzet Baysal University, 14030 Bolu, Türkiye
[c] Department of Pharmaceutical Chemistry, Faculty of Pharmacy, Anadolu University, 26470 Eskişehir, Türkiye
[d] Department of Basic Pharmaceutical Sciences, Faculty of Pharmacy, Çukurova University, Balcalı, 01330 Adana, Türkiye
[e] Department of Biotechnology, Institute of Natural and Applied Sciences, Çukurova University, Balcalı, 01330 Adana, Türkiye

ARTICLE INFO

*Keywords:*
Isoxazole derivatives
Pyridine *N*-oxide
Cycloaddition reaction
Molecular docking study
Monoamine oxidase
Acetylcholinesterase

ABSTRACT

A series of ten novel pyridine *N*-oxide-bearing 5-aminoisoxazoles was efficiently synthesized in moderate yields by reacting 2-(cyanomethyl)pyridine 1-oxide with α-chlorooximes, employing sodium ethoxide as a base. The synthesized compounds were verified with a variety of spectra. Subsequently, the inhibitory potency of compounds **4c, 4e, 4f, 4h**, and **4i** against AChE and BChE, primary targets in Alzheimer's disease, was assessed. In silico docking analyses were conducted to evaluate the interaction of compounds **4c, 4e, 4f, 4h**, and **4i** with AChE and MAO-B. Among the tested compounds, **4e** and **4h** demonstrated remarkable AChE inhibition, exhibiting $IC_{50}$ values of (0.050 μM and 0.039 μM, respectively), comparable to the inhibition achieved by donepezil ($IC_{50}$ = 0.020 μM). Additionally, compounds **4c, 4e, 4f, 4h**, and **4i** displayed potent MAO-A inhibition, with $IC_{50}$ values of (0.203, 0.067, 0.083, 0.044, and 0.159 μM, respectively), surpassing the efficacy of moclobemide ($IC_{50}$ = 6.061 μM). Compounds **4e, 4f**, and **4h** also inhibited MAO-B, with $IC_{50}$ values of (0.076, 0.058, and 0.049 μM, respectively), close to the inhibitory effects of Selegiline ($IC_{50}$ = 0.037 μM). Compound **4h** emerged as a multi-target inhibitor, effectively inhibiting AChE, MAO-A, and MAO-B. These findings underscore the therapeutic potential of these novel compounds in the treatment of Alzheimer's disease, warranting further investigation into their clinical application.

## 1. Introduction

Alzheimer's disease (AD) [1] is a progressive neurodegenerative disorder, characterized by the gradual decline of cognitive, functional, and behavioral abilities, making it the most common form of dementia, especially among the elderly. This condition deeply impacts brain regions responsible for cognitive functions, such as memory, reasoning, and emotional responses, causing significant distress for patients and caregivers alike. With over 55 million individuals affected globally and projections, suggesting a staggering 135 million cases by 2050 due to population aging [2], the urgent need for effective treatments is evident. Currently, there is no cure for AD, highlighting the critical necessity for potent medications capable of slowing or halting its relentless progression. In the field of pharmacology, compounds containing isoxazole are emerging as promising candidates. These compounds have shown promising results across various biological domains [3–6], including cancer, tuberculosis, and neurodegenerative diseases like Parkinson's and Alzheimer's. They act as potent inhibitors of crucial enzymes, notably monoamine oxidases (MAOs) [7–10], which play a pivotal role in neurotransmitter breakdown and are essential targets for neurological conditions. These enzymes, relying on flavin adenine dinucleotide, are situated within the outer mitochondrial membrane of various mammalian cells encompassing glia and neurons. [11] Additionally, isoxazoles have demonstrated remarkable potential as selective inhibitors of acetylcholinesterase (AChE) in vitro studies, showing effectiveness across various species [3,12,13]. This discovery holds

* Corresponding author at: Department of Chemistry, University of Turku, Henrikinkatu 2, 20500 Turku, Finland.
*E-mail address:* lysale@utu.fi (L.Y. Saleh).

https://doi.org/10.1016/j.molstruc.2024.138667
Received 15 January 2024; Received in revised form 30 April 2024; Accepted 16 May 2024
Available online 17 May 2024

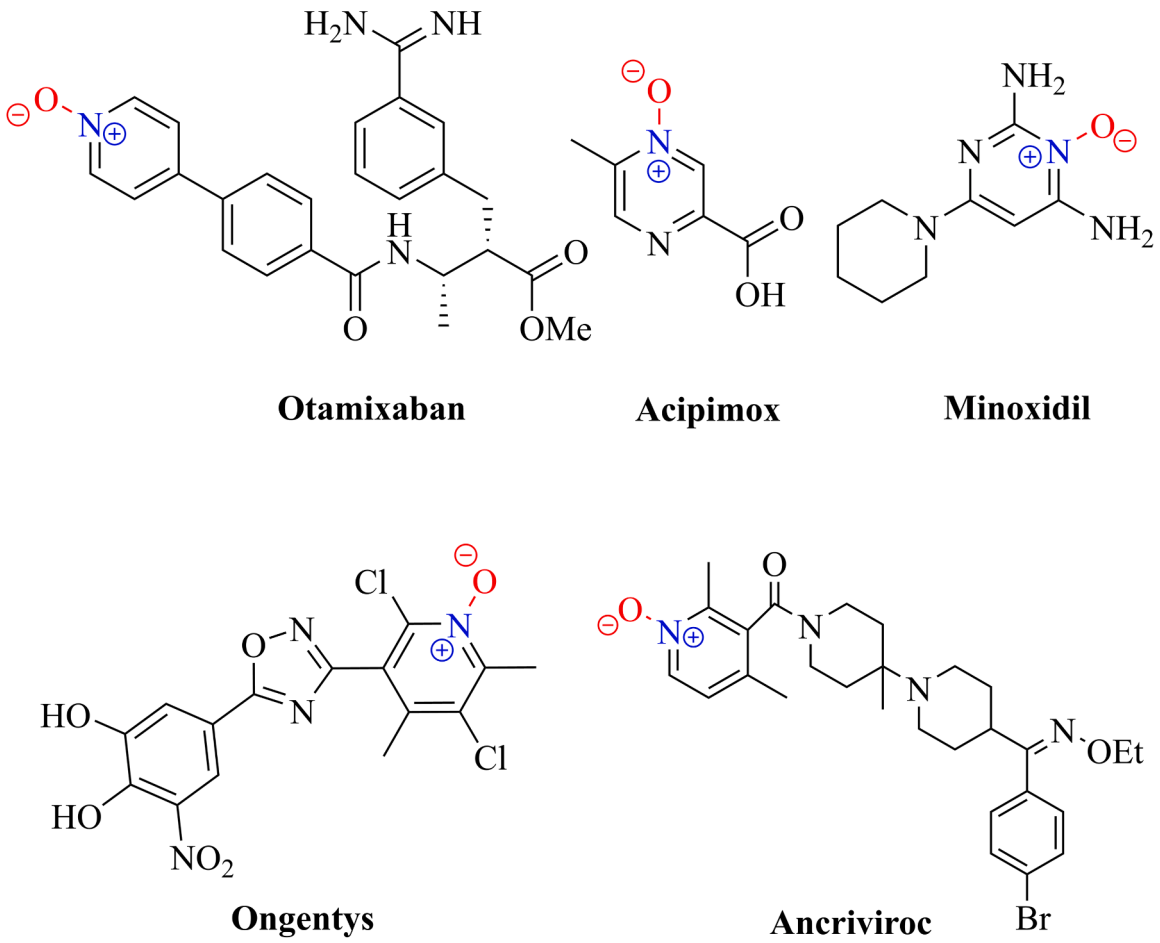


**Fig. 1.** Some chemical structures of *N*-oxide-based drugs.

significant promise for the management of AD.

The synthesis of *N*-oxide and their derivatives [14] has significantly boosted the potential of compounds with *N*-oxide moieties in various biological activities, including antileishmanial, antifungal, antibacterial [15], antiviral [16], and therapeutic agents [17]. Among them, *N*-oxidation of isoxazoles exhibits drug-like properties, particularly in addressing neuropsychiatric disorders [18]. The review explores the therapeutic potential of isoxazoles and their *N*-oxide derivatives, emphasizing their unique mechanisms of action [19], which not only hold promise for addressing neuropsychiatric disorders but also open diverse avenues in drug discovery [17]. In Fig. 1, a visual illustration of various molecules containing *N*-oxide functionalities and their respective roles as therapeutic agents. Notable examples of known drugs include Acipimox, an antilipolytic agent; Minoxidil, an antihypertensive vasodilator; Ongentys, a COMT inhibitor; Otamixaban, an antithrombotic; and Ancriviroc, a CCR5 antagonist.

Current AD treatments, including galantamine, donepezil, and rivastigmine, are cholinesterase inhibitors [20,21]. Donepezil and galantamine selectively target AChE, while rivastigmine inhibits both AChE and butyrylcholinesterase (BChE). The cholinergic system in the brain, crucial for cognitive functions, relies on AChE and BChE enzymes, which hydrolyze acetylcholine [22,23]. AChE inhibitors are preferred for maintaining normal ACh levels due to their superior hydrolytic activity. Previous research highlights AChE's narrow gorge housing five ligand-binding sites [24], including catalytic anionic side (CAS) and peripheral anionic side (PAS) being the primary regions where Trp86, Glu202, Tyr337, Tyr72, Tyr124, Trp286, and Asp74 residues are located [25]. Notably, compounds like donepezil, tacrine dimers, and their analogs bind concurrently to PAS and CAS [26]. Studies suggest AChE inhibitors should have a linker group connecting the basic center and primary ring structure, with options including methylene, oxygen, or amide derivatives [27]. Fig. 2 illustrates a structural comparison among donepezil, rivastigmine, and pyridine *N*-oxide containing 5-aminoisoxazoles. In this comparison, the pyridine *N*-oxide serves as the central basic

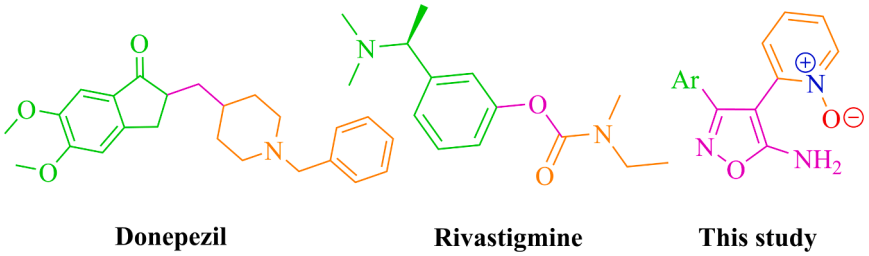


**Fig. 2.** Isoxazole ring as a linker of basic center and aromatic ring.

moiety, while the aromatic substituted serves as the core ring with the isoxazole ring acting as the linker. Having the 5-aminoisoxazole ring as a linker has the potential to augment interactions with related enzymes, owing to its unique structural characteristics.

Building upon the previous work related to the cyclization/cycloaddition of hydroximoyl chlorides with active methylene compounds [28,29] to form hybrid molecules, the synthesis of these novel aromatic-substituted 2-(5-aminoisoxazol-4-yl)pyridine 1-oxides **4a-j** is reported in this study. The research outlined in this paper investigates the efficiency of synthesized compounds, their biological effects, and the computational analysis of interaction mechanisms. The findings have the potential to be extremely valuable and could offer a convenient foundation for the creation of novel MAO-A, MAO-B and AChE inhibitors to combat neurodegenerative disease. This, in turn, may significantly expedite the drug development process.

## 2. Materials and methods

### 2.1. Experimental

Sigma Aldrich provided the commercial chemicals and reagents used in this experiment. Merck silica gel F-254 plates were utilized for analytical thin-layer chromatography (TLC). MELTEMP apparatus was employed to measure the melting points (m.p.) in open capillary tubes and no corrections were made. The synthesized molecules were viewed through UV-4LC. SHIMADZU FT-IR-8400S was used to record Fourier Transform Infrared (FT-IR) spectra. The NMR spectra were obtained at room temperature using Bruker Biospin 500 MHz NMR spectrometer in DMSO-$d_6$, and the chemical shifts are expressed in parts per million (ppm), with the coupling constants (*J*) given in Hertz (Hz). The splitting patterns were assigned as follows: *s* (singlet); *d* (doublet); *m* (multiplet); *dd* (doublets of doublet); *td* (triplets of doublet) (Supplementary data). Lastly, high-resolution mass spectra were performed on a Bruker Daltonics micrOTOF-Q mass spectrometer (Bruker, Billerica, MA, USA) using electrospray ionization.

### 2.2. Procedure for the synthesis of N-oxide intermediate **1**

*m*-Chloro-perbenzoic acid (15 mmol, 2588 mg) was added portionwise into the solution of 2-pyridylacetonitrile (10 mmol, 1181 mg) in dichloromethane and the mixture was stirred at room temperature for four hours. The solvent was evaporated and purified by column chromatography.

#### 2.2.1. 2-(cyanomethyl)pyridine 1-oxide **1**

Light brown solid, (685 mg, 51 %), $R_f$ : (EtOAc: MeOH-7:1) = 0.47, mp = 129–131, $\nu_{max}$ (KBr, $cm^{-1}$): 3051–3024 (Ar-CH), 2935–2906 ($CH_2$), 2249 (C ≡ N). HRMS: required for $C_7H_7N_2O$ [*M* + *H*]+ 135.0558 and found 135.0561. $^1$H NMR (500 MHz, DMSO-$d_6$) δ 8.38 (dd, *J* = 6.4, 0.7 Hz, 1H, PyH5), 7.65 (dd, *J* = 7.8, 2.1 Hz, 1H, PyH3), 7.50 – 7.44 (m, 1H, PyH2), 7.43 – 7.38 (m, 1H, PyH4), 4.15 (s, 2H, $CH_2$). $^{13}$C NMR (126 MHz, DMSO--$d_6$) δ 141.8(PyC1), 139.5(PyC5), 126.8(PyC3), 126.7 (PyC2), 126.0(PyC4), 116.9(C ≡ N), 20.1($CH_2$). *m/z* (TOF ES+) 135 (*M* + *H*).

### 2.3. General procedure for the synthesis of compounds **4a-j**

The solution of the corresponding aryl *N*-hydroximoyl chloride (2 mmol) in ethanol was added dropwise into a stirring solution of 2-(cyanomethyl)pyridine 1-oxide (1 mmol, 134 mg) and sodium metal (60 mg) in 5 mL ethanol at room temperature. After 10 min of stirring, the solvent was evaporated and the crude material was extracted with ethyl acetate and water (30 mL: 30 mL) ×3. The combined organic phase was washed with brine solution, dried with $Na_2SO_4$. The solvent was evaporated under reduced pressure. Finally, the products were recrystallized with ethyl acetate and hexane mixture.

#### 2.3.1. 2-(5-amino-3-(4-chlorophenyl)isoxazol-4-yl)pyridine 1-oxide (**4a**)

Light yellow solid, (168 mg, 59 %), $R_f$ : (EtOAc: MeOH-9:1) = 0.62, mp = 195–197, $\nu_{max}$ (KBr, $cm^{-1}$): 3074 (Ar-CH), 1637 (C═N), 3265 ($NH_2$), HRMS: required for $C_{14}H_{10}ClN_3O_2$ $[M+H]^+$ 288.0540 and found 288.0542. $^1$H NMR (500 MHz, DMSO-$d_6$) δ 8.34 (dd, *J* = 6.5, 0.7 Hz, 1H, PyH5), 7.50 (d, *J* = 8.54 2H, Ph H3 and PhH5), 7.39 (d, *J* = 8.68 2H, Ph H2 and PhH6), 7.34 (s, 2H, $NH_2$), 7.33 – 7.29 (m, 1H, PyH4), 7.23 (td, *J* = 7.8, 1.3 Hz, 1H, PyH3), 6.97 (dd, *J* = 8.0, 1.9 Hz, 1H, PyH2). $^{13}$C NMR (126 MHz, DMSO-$d_6$) δ 169.6(C—$NH_2$), 161.4(Ph-C), 141.6(PyC1), 140.4(PyC5), 135.0(PhC4), 130.1(PhC3 and PhC5), 129.4(PhC2 and PhC6), 128.5(PhC1), 128.1(PyC2), 126.1(PyC3), 124.5(PyC4), 85.6 (PyC). *m/z* (TOF $ES^+$) 290 (*M* + 2).

#### 2.3.2. 2-(5-amino-3-(4-nitrophenyl)isoxazol-4-yl)pyridine 1-oxide (**4b**)

Yellow solid, (207 mg, 69 %), $R_f$ : (EtOAc: MeOH-9:1) = 0.68, mp = 228–230, $\nu_{max}$ (KBr, $cm^{-1}$): 3082 (Ar-CH), 1629 (C═N), 3389 ($NH_2$), HRMS: required for $C_{14}H_{10}N_4O_4$ $[M+H]^+$ 299.0780 and found 299.0786. $^1$H NMR (500 MHz, DMSO-$d_6$) δ 8.34 (dd, *J* = 6.5, 0.7 Hz, 1H, PyH5), 8.25 (d, *J* = 8.89 Hz, 2H, PhH3 and PhH5), 7.66 (d, *J* = 8.90 Hz, 2H, PhH2 and PhH6), 7.41 (s, 2H, $NH_2$), 7.36 – 7.31 (m, 1H, PyH4), 7.26–7.21 (m, 1H, PyH3), 7.05 (dd, *J* = 8.0, 1.8 Hz, 1H, PyH2). $^{13}$C NMR (126 MHz, DMSO-$d_6$) δ 169.8(C—$NH_2$), 160.9(Ph-C), 148.5(PhC4), 141.2(PyC1), 140.4(PyC5), 136.3(PhC3 and PhC5), 129.5(PhC2 and PhC6), 128.3(PhC1), 126.2(PyC3), 124.8(PyC2), 124.4(PyC4), 85.6 (PyC). *m/z* (TOF $ES^+$) 299 (*M* + *H*).

#### 2.3.3. 2-(5-amino-3-(4-bromophenyl)isoxazol-4-yl)pyridine 1-oxide (**4c**)

White solid, (200 mg, 60 %), $R_f$ : (EtOAc: MeOH-9:1) = 0.63, mp = 189–191, $\nu_{max}$ (KBr, $cm^{-1}$): 3063 (Ar-CH), 1631 (C═N), 3232 ($NH_2$), HRMS: required for $C_{14}H_{10}BrN_3O_2$ $[M+H]^+$ 332.0035 and found 332.0042. $^1$H NMR (500 MHz, DMSO-$d_6$) δ 8.34 (dd, *J* = 6.5, 0.7 Hz, 1H, PyH5), 7.63 (d, *J* = 8.55 Hz, 2H, PhH3 and PhH5), 7.36 – 7.28 (m, 5H, PhH2 and PhH6(2H), PyH4(1H), $NH_2$(2H)), 7.23 (td, *J* = 7.8, 1.2 Hz, 1H, PyH3), 6.97 (dd, *J* = 8.0, 1.9 Hz, 1H, PyH2). $^{13}$C NMR (126 MHz, DMSO-$d_6$) δ 169.6(C—$NH_2$), 161.4(Ph-C), 141.6(PyC1), 140.4(PyC5), 132.3(PhC4), 130.3(PhC3 and PhC5), 128.9(PhC2 and PhC6), 128.1 (PhC1), 126.1(PyC2), 124.5(PyC3), 123.7(PyC4), 85.6(Py-C). *m/z* (TOF $ES^+$) 334 (*M* + 2).

#### 2.3.4. 2-(5-amino-3-phenylisoxazol-4-yl)pyridine 1-oxide (**4d**)

Yellowish solid, (200 mg, 60 %), $R_f$ : (EtOAc: MeOH-9:1) = 0.68, mp = 198–200, $\nu_{max}$ (KBr, $cm^{-1}$): 3061 (Ar-CH), 1626 (C = N), 3223 ($NH_2$). HRMS: required for $C_{14}H_{11}N_3O_2$ $[M+H]^+$ 254.0930 and found 254.0933. $^1$H NMR (500 MHz, DMSO-$d_6$) δ 8.35 (d, *J* = 6.0 Hz, 1H, PyH5), 7.49 – 7.40 (m, 3H, PhH3,H4 and PhH5), 7.39–7.35 (m, 2H, PhH2 and PhH6), 7.32 (s, 2H, $NH_2$), 7.31 – 7.26 (m, 1H, PyH4), 7.18 (td, *J* = 7.9, 1.2 Hz, 1H, PyH3), 6.90 (dd, *J* = 8.0, 1.9 Hz, 1H, PyH2). $^{13}$C NMR (126 MHz, DMSO-$d_6$) δ 169.5(C—$NH_2$), 162.4(Ph-C), 142.0 (PyC1), 140.4(PyC5), 130.2(PhC3 and PhC5), 129.6(PhC2 and PhC6), 129.3(PhC4), 128.4(PhC1), 128.0(PyC2), 126.0(PyC3), 124.3(PyC4), 85.8(Py-C). *m/z* (TOF $ES^+$) 254 (*M* + *H*).

#### 2.3.5. 2-(5-amino-3-(2-chloro-4-methoxyphenyl)isoxazol-4-yl)pyridine 1-oxide (**4e**)

Yellowish solid, (158 mg, 50 %), $R_f$ : (EtOAc: MeOH-9:1) = 0.56, mp = 221–223, $\nu_{max}$ (KBr, $cm^{-1}$): 3099–3012 (Ar-CH), 2976–2941 ($CH_2$), 1641 (C═N), 3252 ($NH_2$). HRMS: required for $C_{15}H_{13}ClN_3O_3$ $[M+H]^+$ 318.0645 and found 318.0654. $^1$H NMR (500 MHz, DMSO-$d_6$) δ 8.35 (dd, *J* = 11.2, 5.3 Hz, 1H,PyH5), 7.43 (d, *J* = 2.1 Hz, 1H, PhH3), 7.35 – 7.26 (m, 4H, PH5(1H),Ph6(1H) and $NH_2$(2H)), 7.24 (td, *J* = 7.9, 1.2 Hz, 1H, PyH4), 7.19 (d, *J* = 8.6 Hz, 1H, PyH3), 7.01 (dd, *J* = 8.0, 1.9 Hz, 1H, PyH2), 3.88 (s, 3H, $OCH_3$). $^{13}$C NMR (126 MHz, DMSO-$d_6$) δ 169.5 (C—$NH_2$), 160.9(pH—C), 156.0(PhC4), 141.8(PyC1), 140.4(PyC5), 129.4(PhC6), 128.5(PhC5), 128.2(PyC2), 126.1(PyC3), 124.5(PyC4), 122.7(PhC1), 121.8(Ph3), 113.5(Ph2), 85.5(Py-C), 56.7($OCH_3$). *m/z* (TOF $ES^+$) 320 (*M* + 2).

*2.3.6. 2-(5-amino-3-(2-chloro-4,5-dimethoxyphenyl)isoxazol-4-yl) pyridine 1-oxide (**4f**)*

White solid, (179 mg, 52 %), $R_f$ : (EtOAc: MeOH-9:1) = 0.59, mp = 212–214, $\nu_{max}$ (KBr, $cm^{-1}$): 3055 (Ar-CH), 2931 ($CH_2$) 1639 (C═N), 3236 ($NH_2$). HRMS: required for $C_{16}H_{15}ClN_3O_4$ $[M+H]^+$ 348,0751 and found 348.0762. $^1$H NMR (500 MHz, DMSO-$d_6$) δ 8.32 (d, $J$ = 5.9 Hz, 1H, PyH5), 7.37 (s, 2H, $NH_2$), 7.25 (td, $J$ = 7.1, 2.0 Hz, 1H, PyH4), 7.18 (td, $J$ = 7.9, 1.2 Hz, 1H, PyH3), 7.12 (s, 1H, PhH3), 7.07 (s, 1H, PhH6), 6.78 (dd, $J$ = 8.1, 1.9 Hz, 1H, PyH2), 3.81 (s, 3H, Ph-p–$OCH_3$), 3.79 (s, 3H, Ph-m–$OCH_3$). $^{13}$C NMR (126 MHz, DMSO-$d_6$) δ 169.0(C—$NH_2$), 161.0(pH—C), 150.8(PhC5), 148.3(PhC4), 142.2(PyC1), 140.3(PyC5), 126.5(PyC2), 125.7(PyC3), 124.0(PyC4), 123.8(PhC1), 120.0(PhC3), 114.4(PhC6), 113.5(PhC2), 87.8(Py-C), 56.5(pH-p–$OCH_3$), 56.3(Ph-m–$OCH_3$). $m/z$ (TOF $ES^+$) 350 ($M$ + 2).

*2.3.7. 2-(5-amino-3-(4-fluorophenyl)isoxazol-4-yl)pyridine 1-oxide (**4g**)*

Yellow solid, (180 mg, 66 %), $R_f$ : (EtOAc: MeOH-9:1) = 0.65, mp = 185–187, $\nu_{max}$ (KBr, $cm^{-1}$): 3074 (Ar-CH), 1647 (C═N), 3267 ($NH_2$). HRMS: required for $C_{14}H_{10}FN_3O_2$ $[M + H]^+$ 272.0835 and found 272.0840. $^1$H NMR (500 MHz, DMSO-$d_6$) δ 8.35 (d, $J$ = 6.1 Hz, 1H, PyH5), 7.43 (d, $J$ =,8.81 Hz, 2H, PhH3 and PhH5), 7.32 (s, 2H, $NH_2$), 7.31 – 7.24 (m, (1H) PhH2, (1H) PhH6 and (1H) PyH4), 7.21 (td, $J$ = 7.9, 1.0 Hz, 1H, PyH3), 6.94 (dd, $J$ = 8.0, 1.9 Hz, 1H, PyH2). $^{13}$C NMR (126 MHz, DMSO-$d_6$) δ 169.6(C—$NH_2$), 163.3 (d, $^1J_{C\text{-}F}$ = 246.9 Hz), 161.5 (pH—C), 141.8(PyC1), 140.4(PyC5), 130.7 (d, $^3J_{C\text{-}F}$ = 8.6 Hz), 128.1 (PyC2), 126.1 (d, $^4J_{C\text{-}F}$ = 3.2 Hz), 126.0(PyC3), 124.4(PyC4), 116.4 (d, $^2J_{C\text{-}F}$ = 21.8 Hz). 85.7(Py-C). $m/z$ (TOF $ES^+$) 272 ($M$ + $H$).

*2.3.8. 2-(5-amino-3-(2,4-dichlorophenyl)isoxazol-4-yl)pyridine 1-oxide (**4h**)*

White solid, (181 mg, 57 %), $R_f$ : (EtOAc: MeOH-9:1) = 0.71, mp = 226–228, $\nu_{max}$ (KBr, $cm^{-1}$): 3066 (Ar-CH), 1647 (C═N), 3248 ($NH_2$). HRMS: required for $C_{14}H_9Cl_2N_3O_2$ $[M + H]^+$ 322.0150 and found 322.0158. $^1$H NMR (500 MHz, DMSO-$d_6$) δ 8.31 (d, $J$ = 6.4 Hz, 1H, PyH5), 7.72 (d, $J$ = 1.8 Hz, 1H, PhH5), 7.65 – 7.52 (m, 2H, PhH3 and PhH6), 7.42 (s, 2H, $NH_2$), 7.31 – 7.22 (m, 1H, PyH4), 7.19 (dd, $J$ = 11.4, 4.1 Hz, 1H, PyH3), 6.77 (dd, $J$ = 8.0, 1.7 Hz, 1H, PyH2). $^{13}$C NMR (126 MHz, DMSO-$d_6$) δ 169.2(C—$NH_2$), 160.2(Ph-C), 141.8(PyC1), 140.3 (PyC5), 135.9(PhC4), 133.7(PhC2), 133.4(PhC3), 130.1(PhC5), 128.5 (PhC1), 127.9(PyC2), 126.4(PyC3), 125.8(PhC6), 124.1(PyC4), 87.6 (Py-C). $m/z$ (TOF $ES^+$) 324 ($M$ + 2).

*2.3.9. 2-(5-amino-3-(2,6-dichlorophenyl)isoxazol-4-yl)pyridine 1-oxide (**4i**)*

Light yellow solid, (145 mg, 45 %), $R_f$ : (EtOAc: MeOH-9:1) = 0.72, mp = 240–242, $\nu_{max}$ (KBr, $cm^{-1}$): 3082 (Ar-CH), 1658 (C═N), 3255 ($NH_2$). HRMS: required for $C_{14}H_9Cl_2N_3O_2$ $[M+H]^+$ 322.0150 and found 322.0158. $^1$H NMR (500 MHz, DMSO-$d_6$) δ 8.32 (d, $J$ = 6.4 Hz, 1H, PyH5), 7.69 – 7.60 (m, 2H, PhH3 and PhH5), 7.56 (dd, $J$ = 8.9, 7.1 Hz, 1H, PhH4), 7.47 (s, 2H, $NH_2$), 7.25 (dd, $J$ = 9.7, 3.9 Hz, 1H, PyH4), 7.17 (dd, $J$ = 17.1, 9.4 Hz, 1H, PyH3), 6.70 (d, $J$ = 7.9 Hz, 1H, PyH2). $^{13}$C NMR (126 MHz, DMSO-$d_6$) δ 169.4(C—$NH_2$), 158.5(Ph-C), 141.2 (PyC1), 140.5(PyC5), 135.1(PhC2 and PhC6), 133.0(PhC3 and PhC5), 129.3(PhC1), 128.0(PyC2), 126.6(PyC3), 124.7(PhC4), 124.0(PyC4), 87.4(Py-C). $m/z$ (TOF $ES^+$) 324 ($M$ + 2).

*2.3.10. 2-(5-amino-3-(p-tolyl)isoxazol-4-yl)pyridine 1-oxide (**4j**)*

White solid, (126 mg, 47 %), $R_f$ : (EtOAc: MeOH-9:1) = 0.59, mp = 209–211, $\nu_{max}$ (KBr, $cm^{-1}$): 3093–3063 (Ar-CH), 2924 ($CH_2$) 1635 (C = N), 3232 ($NH_2$). HRMS: required for $C_{15}H_{13}N_3O_2$ $[M + H]^+$ 268.1086 and found 268.1094. $^1$H NMR (500 MHz, DMSO-$d_6$) δ 8.35 (d, $J$ = 6.5 Hz, 1H PyH5), 7.32 – 7.21 (m, PyH4(1H), $NH_2$(2H),PhHs(4H)), 7.19 (td, $J$ = 7.9, 1.2 Hz, 1H, PyH3), 6.90 (dd, $J$ = 8.0, 1.9 Hz, 1H PyH2), 2.33 (s, 3H, $CH_3$). $^{13}$C NMR (126 MHz, DMSO-$d_6$) δ 169.5($CNH_2$), 162.2(PhC), 142.1(PyC1), 140.4(PyC5), 139.8(PhC2 and PhC6), 129.9(PhC3 and PhC5), 128.3(PhC1), 128.0(PyC2), 126.6(PhC4), 126.0(PyC3), 124.2 (PyC4), 85.7(Py-C), 21.4($CH_3$). $m/z$ (TOF $ES^+$) 268 ($M$ + $H$).

**Table 1**
$^{13}$C NMR peaks for compounds **4a-j**.

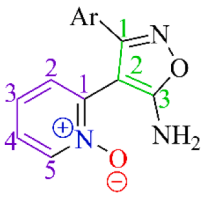


| Carbon atoms on the molecules | $^{13}$C NMR chemical shift (ppm) |
|---|---|
| Isoxazole **C1** | 160.2–162.4 |
| Isoxazole **C2** | 85.6–87.8 |
| Isoxazole **C3** | 169.0–169.8 |
| Pyridine **C1** | 140.3–140.4 |
| Pyridine **C2** | 126.5–128.6 |
| Pyridine **C3** | 125.7–126.6 |
| Pyridine **C4** | 124.0–124.5 |
| Pyridine **C5** | 141.2–142.2 |

## 3. Results and discussion

### 3.1. Chemistry

The present study describes the preparation and characterization of a series of novel aromatic substituted 2-(5-aminoisoxazol-4-yl)pyridine 1-oxides **4a-j**. The compounds were synthesized *via* the reaction of 2-(cyanomethyl)pyridine 1-oxide with the corresponding aryl *N*-hydroximoyl-chlorides in ethanol, using freshly prepared sodium ethoxide as the base. The resulting compounds were purified by recrystallization and characterized by various spectroscopic techniques. The characterization data obtained from $^1$H and $^{13}$C NMR, mass spectrometry, and infrared spectroscopy confirm the successful synthesis and structure of compounds **4a-j**. The $^1$H NMR spectra showed broad singlets in the range of 7.2–7.4 ppm corresponding to the amine protons $NH_2$, while the remaining protons signals were observed within their usual chemical shifts. The carbon peaks were also consistent with the expected structures of the compounds, as summarized in Table 1.

The synthesis strategy used in this study, which involves the oxidation of pyridine to produce a very stable active methylene, was effective in increasing the pyridinyl proton acidity, enabling its deprotonation using freshly prepared sodium ethoxide as the base. This approach avoids the use of strong bulky bases *t*-BuOK or LDA [30], which could have resulted in unwanted side reactions. The prepared compounds **4a-j** could potentially have interesting biological activities and could serve as valuable intermediates for the synthesis of various bioactive compounds. Overall, this study contributes to the development of new methods for the synthesis of isoxazole-containing heterocyclic compounds, and provides useful insights into the reactivity of pyridine derivatives towards *N*-hydroximoyl chlorides (Table 2).

The study reported successful chlorination of aldoximes using an excess of *N*-chlorosuccinimide (NCS) in DMF. Notably, the chlorination of 4-methoxybenzaldehyde and 3,4-dimethoxybenzaldehyde oximes resulted in substitution of both the iminic carbon and the aromatic rings at the ortho-position. This finding is significant as it highlights the potential of using excess NCS to achieve substitution at multiple sites in organic molecules.

The supplementary material on compounds **4e** and **4f** provides further evidence of the effectiveness of this approach. While the exact mechanism of novel compounds **4a-j** remains uncertain, the experimental results suggest a possible mechanistic pathway, as illustrated in Scheme 1. Firstly, the base initiates the removal of hydrogen on the active methylene group, resulting in the formation of a carbon anion. The anion then reacts with the in situ formed nitrile oxide. Secondly,

**Table 2**
Reaction schemes, isolated yields[a] and melting points of **4a-j**.

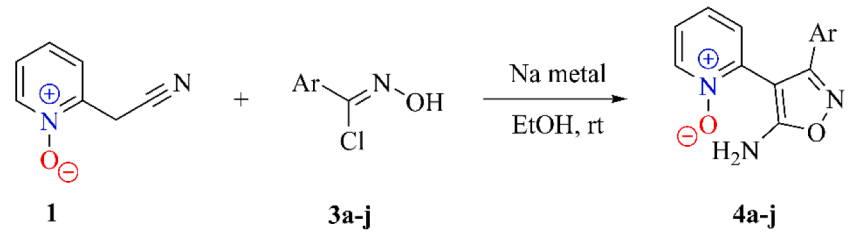


| Entry | Ar | [a]Yield (%) | m.p. (°C) |
|---|---|---|---|
| **4a** | 4-$ClC_6H_4$ | 59 | 195–197 |
| **4b** | 4-$NO_2C_6H_4$ | 69 | 228–230 |
| **4c** | 4-$BrC_6H_4$ | 60 | 189–191 |
| **4d** | $C_6H_5$ | 60 | 198–200 |
| **4e** | 2-Cl-4-MeO-$C_6H_3$ | 50 | 221–223 |
| **4f** | 2-Cl-4,5-DiMeO$C_6H_2$ | 52 | 212–214 |
| **4g** | 4-$FC_6H_4$ | 66 | 185–187 |
| **4h** | 2,4-$Cl_2C_6H_3$ | 57 | 226–228 |
| **4i** | 2,6-$Cl_2C_6H_3$ | 45 | 240–242 |
| **4j** | 4-$MeC_6H_4$ | 47 | 209–211 |

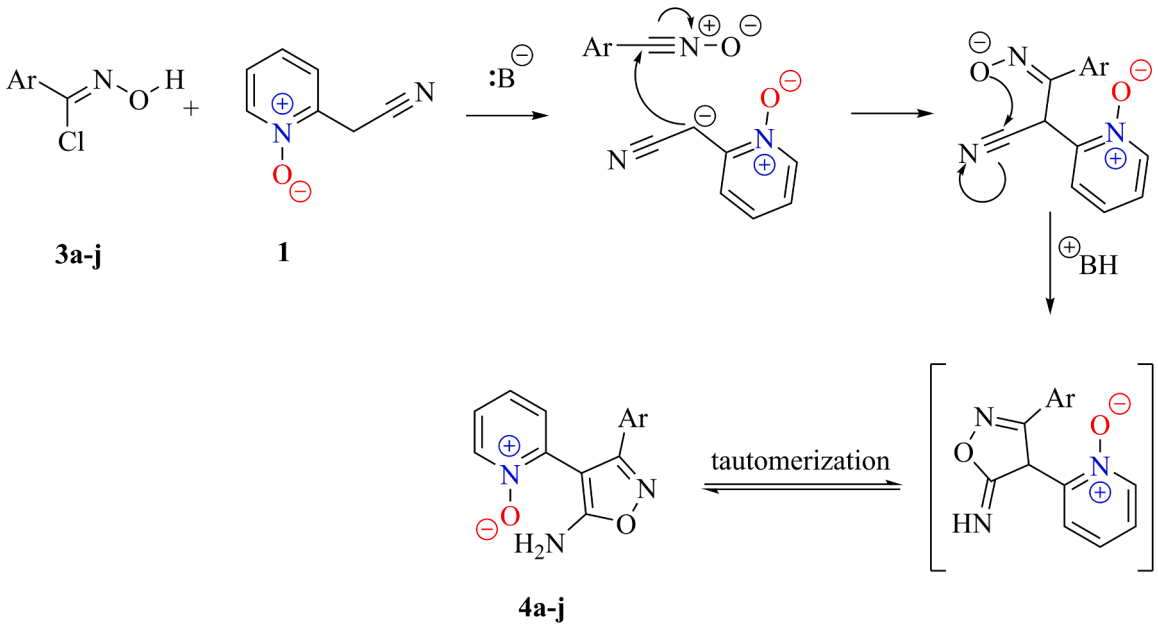


**Scheme 1.** A proposed mechanism towards the formation of pyridine-*N*-oxides containing 5-aminoisoxazoles.

oxygen intermolecularly attacks the electrophilic carbon of the nitrile, resulting in the formation of a cyclic intermediate. Finally, the intermediate undergoes tautomerization, leading to the formation of 5-aminoisoxazoles **4a-j**. This proposed mechanism provides a useful framework for understanding the transformation, although further investigation is needed to confirm its validity.

### 3.2. *In vitro ChE enzymes inhibition assay*

Utilizing the modified Ellman approach as detailed in several, research studies [32–35], the inhibitory activities of these compounds (**4c, 4e, 4f, 4h and 4i**) against AChE and BChE were assessed. Human AChE (CAS No. 9000-81-1) and human BChE (CAS No. 9001-08-5) were employed as the enzymatic targets in the experiments, with donepezil and tacrine serving as the reference drugs. Tacrine, the pioneering AChE inhibitor used in clinical settings, was withdrawn from the market due to hepatotoxicity. Despite the availability of drugs such as donepezil, galantamine, and rivastigmine, their efficacy remains limited. Consequently, the pursuit of novel (AD) drug candidates continues to be a prominent research area [36–38].

As depicted in Table 3, the AChE and BChE inhibitory activities of the selected compounds were evaluated against human AChE and BChE enzymes. The results revealed that compound **4e** and **4h** exhibited the most potent inhibition against AChE, with $IC_{50}$ values of 0.050 ± 0.002 and 0.039 ± 0.001 μM respectively. While compound **4c, 4f and 4i** demonstrated less activity with $IC_{50}$ values of 0.255 ± 0.010, 0.116 ± 0.004 and 0.228 ± 0.011 μM respectively, when compared to the control drug donepezil with an $IC_{50}$ value of 0.0201 ± 0.0001 μM. However, all the tested compounds displayed weak or negligible inhibition against BChE, with $IC_{50}$ values greater than 100 μM, when compared with tacrine the control with an $IC_{50}$ of 0.0064 ± 0.0002 μM. To sum up, optimizing the aryl group of these compounds has the potential to augment their inhibitory activity against AChE, and potentially BChE, making them promising candidates for further exploration. However,

**Table 3**
$IC_{50}$ value of the selected compounds against the AChE, BChE, MAO-A and MAO-B enzymes.

| Compounds | $IC_{50}$ values (μM) | | | |
|---|---|---|---|---|
| | AChE enzyme | BChE enzyme | MAO-A enzyme | MAO-B enzyme |
| **4c** | 0.255 ± 0.010 | >1000 | 0.203 ± 0.009 | 0.128 ± 0.005 |
| **4e** | 0.050 ± 0.002 | >100 | 0.067 ± 0.002 | 0.076 ± 0.003 |
| **4f** | 0.116 ± 0.004 | >100 | 0.083 ± 0.003 | 0.058 ± 0.002 |
| **4h** | 0.039 ± 0.001 | >100 | 0.044 ± 0.002 | 0.049 ± 0.002 |
| **4i** | 0.228 ± 0.011 | >1000 | 0.159 ± 0.007 | 0.195 ± 0.009 |
| **Donepezil** | 0.0201 ± 0.0001 | – | – | – |
| **Tacrine** | – | 0.0064 ± 0.0002 | – | – |
| **Moclobemide** | – | – | 6.0613 ± 0.262 | – |
| **Selegiline** | – | – | – | 0.0374 ± 0.0016 |

the observed limited efficacy against BChE indicates a preference for AChE as the primary enzymatic target.

### 3.3. In vitro MAO enzymes inhibition assay

The fluorometric methodology, as delineated in previous reports [39–42], was utilized to assess the inhibitory effects of the synthesized compounds **4c, 4e, 4f, 4h**, and **4i** against MAO-A and MAO-B. Recombinant human MAO-A and MAO-B enzymes with moclobemide and Selegiline serving as the reference drugs. Both moclobemide and selegiline are considered second-generation monoamine oxidase inhibitor (MAOI), which are generally safer than the much older, non-selective MAOIs. They are associated with a lower risk of dietary restrictions compared to the older MAOIs. However, they still require careful monitoring, and individuals taking these medications should be aware of potential interactions with certain foods and other medications [43, 44], which could lead to uncertain implications and health challenges. Hence, the investigation into alternatives is centered on identifying potential drugs that do not induce adverse reactions or negative interactions with food or other medications.

Table 3 illustrates the evaluation of MAO-A and MAO-B inhibitory activities for the selected compounds against human MAO-A and MAO-B enzymes. Notably, **4h, 4e**, and **4f** exhibit lower $IC_{50}$ values of 0.044 ± 0.002, 0.067 ± 0.002, and 0.083 ± 0.003 μM, respectively, compared to **4i** and **4c**, which have $IC_{50}$ values of 0.159 ± 0.007 and 0.203 ± 0.009 μM. This suggests that **4h, 4e**, and **4f** have more potent inhibitors of MAO-A than **4i** and **4c**. Furthermore, the control drug moclobemide has a significantly higher $IC_{50}$ value of 6.0613 ± 0.262 μM, indicating lower potency against MAO-A. Thus, these selected compounds emerge as promising candidates for MAO-A inhibition. For MAO-B studies, **4h, 4f**, and **4e** display $IC_{50}$ values of 0.049 ± 0.002, 0.058 ± 0.002, and 0.076 ± 0.003 μM, respectively, with **4h** exhibiting the lowest $IC_{50}$ value among the tested compounds. This suggests that **4h** is the most potent inhibitor of MAO-B, closely approaching the potency of Selegiline, a control drug, which has the lowest $IC_{50}$ value of 0.0374 ± 0.0016 μM. Compounds **4c** and **4i** with $IC_{50}$ values of 0.128 ± 0.005 and 0.195 ± 0.009 μM, respectively, also show notable potency against MAO-B. To sum up, the compounds demonstrate varying degrees of potency against both MAO-A and MAO-B, with some exhibiting stronger inhibitory effects. Comparatively, the control drugs Moclobemide and Selegiline serve as references, with the $IC_{50}$ values of the selected compounds being lower than that of moclobemide. Although their $IC_{50}$ values are higher than Selegiline, they particularly stand out for their potency against MAO-B.

### 3.4. In silico docking between AChE/MAO-B and compounds *4(c-e-f-h-i)*

Prior to conducting the docking studies, the 10 molecules included in this study were evaluated for their potential as drugs based on the Lipinski rule Table 4. Only those molecules that adhered to this rule were selected for the docking process. Additionally, the molecules that conformed to the Lipinski rule were compared based on their logP, molecular weight, H-acceptor, H-donor, number of aromatic rings, and rotatable bonds. The Lipinski rule of five is a useful tool in identifying drug-like compounds and differentiating them from non-drug-like compounds. It predicts the likelihood of success or failure for compounds that follow two or more of the rules due to their drug-like characteristics [31].

- These filters can assist in early preclinical development and potentially prevent expensive failures in late-stage preclinical and clinical trials.
- Compounds with a lower lipophilicity, characterized by a logP value of less than 3.4, are generally expected to exhibit high absorption rates. In contrast, highly lipophilic compounds tend to undergo rapid metabolism, which can result in low solubility, decreased absorption, and high turnover. Extremely high levels of lipophilicity may even cause toxicity and metabolic clearance issues [51].
- The compounds **4c, 4e, 4f, 4h**, and **4i**, not highlighted in red in Table 4, were utilized as ligands during the docking protocol.

DeepSite was used to identify the binding pockets of the enzymes [45] and the location of the ligand that was co-crystallized with the

**Table 4**
Properties of compounds according to Lipinski rule [31].

| Ligand | Mw (g/mol) | LogP (high lipophilicity) | H-bond donors | H-bond acceptors | Molar refractivity |
|---|---|---|---|---|---|
| **4a** | 287,5 | 1,22 | 2 | 4 | 73,00 |
| **4b** | 298,0 | 0,48 | 2 | 6 | 74,64 |
| **4c** | 331,0 | 2,28 | 2 | 4 | 77,66 |
| **4d** | 253,0 | 0,57 | 2 | 4 | 67,98 |
| **4e** | 317,5 | 1,76 | 2 | 5 | 81,06 |
| **4f** | 347,5 | 1,73 | 2 | 6 | 87,03 |
| **4g** | 271,0 | 0,71 | 2 | 4 | 67,94 |
| **4h** | 322,0 | 2,52 | 2 | 4 | 79,53 |
| **4i** | 322,0 | 2,53 | 2 | 4 | 79,53 |
| **4j** | 267,0 | 0,88 | 2 | 4 | 72,72 |

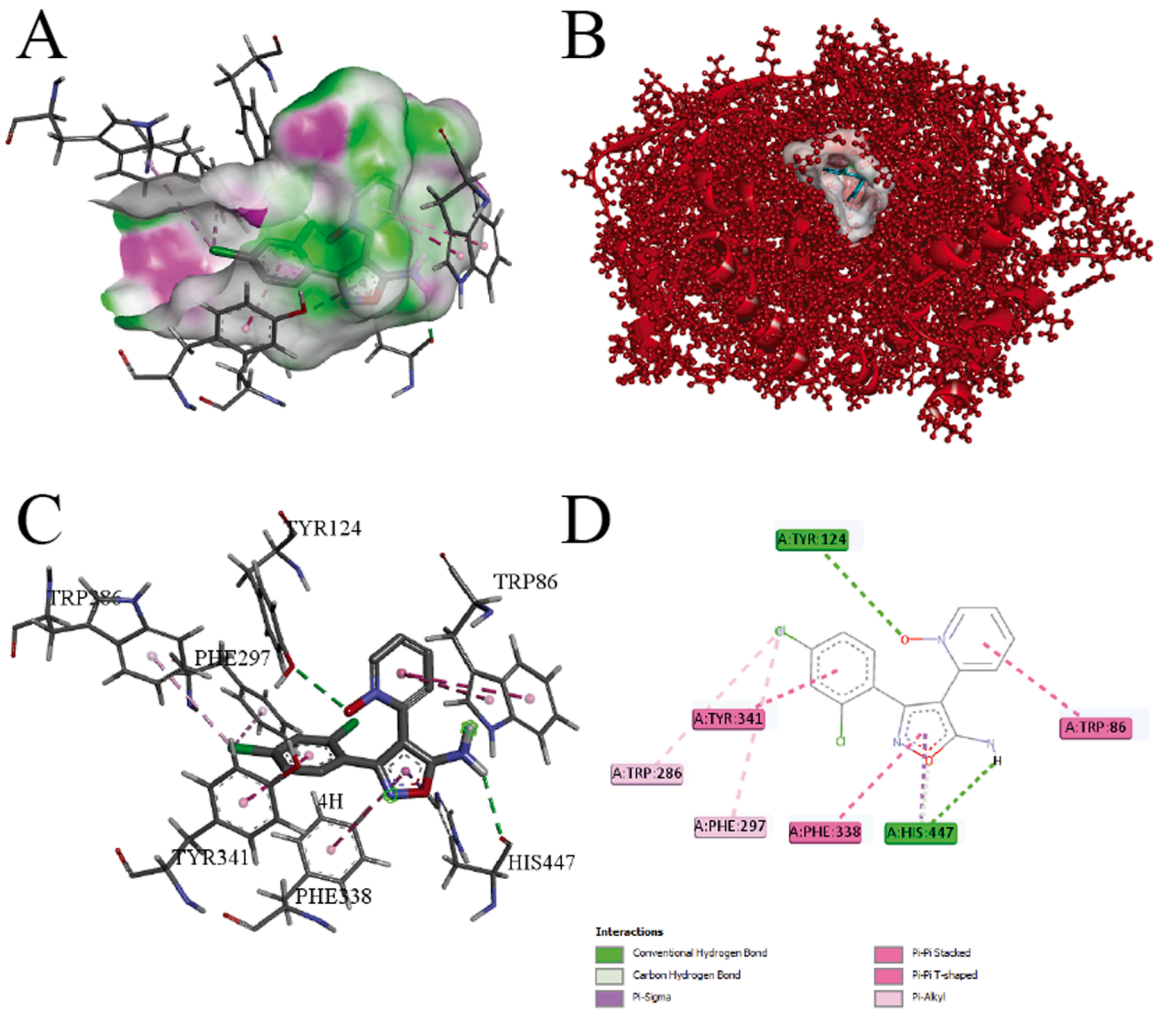


**Fig. 3.** A) Hydrogen donor-acceptor interactions in the pocket region of AChE with **4h**. B) Position of ligand **4h** in the pocket region of AChE. C) 3D diagram of ligand **4h** interaction with AChE residues. D) 2D diagram of **4h** interactions.

complex file can be determined by examining the deposited file in the Protein Data Bank (PDB; www.rcsb.org) [46] accession no: 2V5Z and 4EY7 [47].

Molecular docking is a widely used technique for modeling and monitoring binding free energy and investigate interactions. The process involves utilizing a scoring function to evaluate the sum of both intermolecular and intramolecular interactions within the Autodock Vina algorithm [48]. Autodock Vina's calculation algorithm evaluates the Gibbs free energy of the ligands based on their binding affinity [49]. To conduct further analysis and investigate detailed interactions, Biova Discovery Studio[BIOVIA, Dassault Systèmes, [Discovery Studio Visualizer], [v21.1.0.20298], San Diego: Dassault Systèmes, 2021] and Chimera [50] were also utilized.

### 3.5. Molecular docking study

The docking protocols used in this study were tested and approved by Stefano forli and his colleagues [52]. The results demonstrate that compounds **4h** and **4i** exhibit the highest binding affinities, corroborating the findings of the *in vitro* study on Table 3. In general, the interactions of compounds **4c, 4e, 4f, 4h**, and **4i** with the pocket region of the AChE enzyme reveal consistent patterns: Trp-A: 86 invariably interacts with the pyridine ring, Tyr-A: 124 interacts with the oxygen of amine oxide, and Tyr-A: 341 interacts with the substituted phenyl group. These interactions are similar to donepezil. Moreover, Phe-A: 338 and His-A: 447 which are part of catalytic triad of AChE, interact with the isoxazole ring. Additionally, residues Trp-A: 286, Phe-A: 297, and Gly-A exhibit variable interactions with halogens attached to the phenyl group. Detailed interactions are illustrated in Fig. 3 (Table 5).

**Table 5**
Docking results between AChE and MAO-B with the compounds **4c, 4e, 4f, 4h**, and **4i**.

| Compounds | Binding affinity with AChE (Kcal/mol) | Binding affinity with MAO-B (Kcal/mol) |
|---|---|---|
| **4c** | –9.2 | –8.60 |
| **4e** | –9.2 | –7.20 |
| **4f** | –9.5 | –4.90 |
| **4h** | –10.4 | –7.3 |
| **4i** | –10.8 | –5.1 |
| **Donepezil** | –11.9 | |
| **Safinamide** | | –10.1 |

Regarding the MAO-B enzyme, compounds **4c, 4e, 4f, 4h**, and **4i** exhibit multiple interactions. Cys 172 and Leu 171 formed conventional hydrogen bonds with the oxygen of amine oxide. Tyr 398 had a pi–pi stacked interaction with isoxazole. Flavosine adenosine dinucleotide (FAD) forms pi–alkyl interaction with the pyridine ring. The interactions of these residues are similar to safinamide. The reason for the docking score being lower than expected is that the important residues Gln 206 and Phe 343 are not interacted with **4c, 4e, 4f, 4h**, and **4i**. Detailed interactions are illustrated in Fig. 4. In summary, the inclusion of the

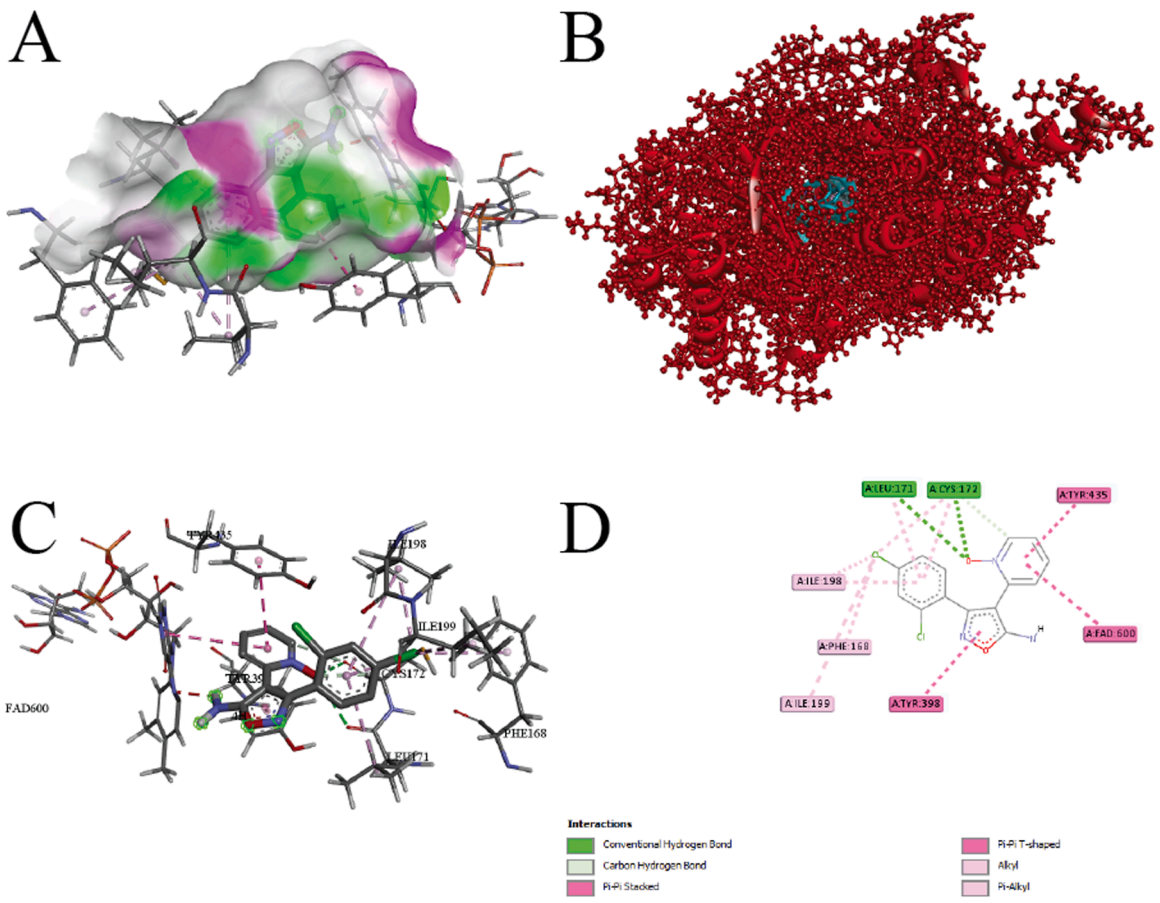


**Fig. 4.** A) Hydrogen donor-acceptor interactions in the pocket region of MAO-B with **4h**. B) Position of **4h** in the pocket region of MAO-B. C) 3D diagram of **4h** interactions with MAO-B residues. D) 2D diagram of **4h** interactions.

isoxazole ring as a linker enhances interactions in the pocket regions of both AChE and MAO-B enzymes.

## 4. Conclusion

In the study, a novel series of ten pyridine *N*-oxide-bearing 5-amino-isoxazoles yielded moderate results. Compounds **4c, 4e, 4f, 4h**, and **4i** showed potent inhibition of MAO-A, surpassing Moclobemide. Compounds **4e, 4f**, and **4h** also inhibited MAO-B, while **4e** and **4i** inhibited AChE. Compound **4h** emerged as a multi-targeting MAO-A, MAO-B, and AChE inhibitor, as indicated by in silico docking analysis with MAO-B and AChE. These compounds show promise in AD treatment, opening avenues for potential therapeutic applications.

## CRediT authorship contribution statement

**Lange Yakubu Saleh:** Writing – review & editing, Writing – original draft, Validation, Methodology, Investigation, Formal analysis, Data curation. **Soner Özdemir:** Writing – review & editing, Writing – original draft, Investigation, Formal analysis, Data curation. **Begüm Nurpelin Sağlık:** Writing – review & editing, Writing – original draft, Investigation, Formal analysis, Data curation. **H. Ali Döndaş:** Writing – review & editing, Writing – original draft, Formal analysis. **Cevher Altug:** Writing – review & editing, Writing – original draft, Visualization, Validation, Supervision, Project administration, Methodology, Investigation, Formal analysis, Data curation, Conceptualization.

## Declaration of competing interest

The authors declare that they have no known competing financial interests or personal relationships that could have appeared to influence the work reported in this paper.

## Data availability

Data will be made available on request.

## Acknowledgments

Molecular graphics and analyses performed with UCSF Chimera, developed by the Resource for Biocomputing, Visualization, and Informatics at the University of California, San Francisco, with support from NIH P41-GM103311.

## Supplementary materials

Supplementary material associated with this article can be found, in the online version, at doi:10.1016/j.molstruc.2024.138667.

## References

[1] M.A. DeTure, D.W. Dickson, The neuropathological diagnosis of Alzheimer's disease, Mol. Neurodegener. 14 (2019) 32, https://doi.org/10.1186/s13024-019-0333-5.
[2] S. Gauthier, C. Webster, S. Servaes, J.A. Morais, Pedro Rosa-Neto, World Alzheimer Report 2022: life after diagnosis: navigating treatment, care and support, 2022.
[3] M. Gutiérrez, M.F. Matus, T. Poblete, J. Amigo, G. Vallejos, L. Astudillo, Isoxazoles: synthesis, evaluation and bioinformatic design as acetylcholinesterase inhibitors, J. Pharmacy Pharmacol. 65 (2013) 1796–1804, https://doi.org/10.1111/jphp.12180.

[4] A. Sysak, B. Obmińska-Mrukowicz, Isoxazole ring as a useful scaffold in a search for new therapeutic agents, Eur. J. Med. Chem. 137 (2017) 292–309, https://doi.org/10.1016/j.ejmech.2017.06.002.

[5] N. Agrawal, P. Mishra, The synthetic and therapeutic expedition of isoxazole and its analogs, Med. Chem. Res. 27 (2018) 1309–1344, https://doi.org/10.1007/s00044-018-2152-6.

[6] C.P. Pandhurnekar, H.C. Pandhurnekar, A.J. Mungole, S.S. Butoliya, B.G. Yadao, A review of recent synthetic strategies and biological activities of isoxazole, J. Heterocycl. Chem. 60 (2023) 537–565, https://doi.org/10.1002/jhet.4586.

[7] N. Agrawal, P. Mishra, Novel isoxazole derivatives as potential antiparkinson agents: synthesis, evaluation of monoamine oxidase inhibitory activity and docking studies, Med. Chem. Res. 28 (2019) 1488–1501, https://doi.org/10.1007/s00044-019-02388-4.

[8] A. Shetnev, A. Kotov, A. Kunichkina, I. Proskurina, S. Baykov, M. Korsakov, A. Petzer, J.P. Petzer, Monoamine oxidase inhibition properties of 2,1-benzisoxazole derivatives, Mol. Divers. (2023), https://doi.org/10.1007/s11030-023-10628-4.

[9] K. Singh, R. Pal, S.A. Khan, B. Kumar, M.J. Akhtar, Insights into the structure activity relationship of nitrogen-containing heterocyclics for the development of antidepressant compounds: an updated review, J. Mol. Struct. 1237 (2021) 130369, https://doi.org/10.1016/j.molstruc.2021.130369.

[10] N. Agrawal, P. Mishra, Synthesis, monoamine oxidase inhibitory activity and computational study of novel isoxazole derivatives as potential antiparkinson agents, Comput. Biol. Chem. 79 (2019) 63–72, https://doi.org/10.1016/j.compbiolchem.2019.01.012.

[11] K.F. Tipton, Enzymology of monoamine oxidase, Cell Biochem. Funct. 4 (1986) 79–87, https://doi.org/10.1002/cbf.290040202.

[12] F. Vafadarnejad, M. Saeedi, M. Mahdavi, A. Rafinejad, E. Karimpour-Razkenari, B. Sameem, M. Khanavi, T. Akbarzadeh, Novel indole-isoxazole hybrids: synthesis and in vitro anti-cholinesterase activity, Lett. Drug Des. Discov. 14 (2017), https://doi.org/10.2174/1570180813666161018124726.

[13] A. Rastegari, M. Safavi, F. Vafadarnejad, Z. Najafi, R. Hariri, S.N.A. Bukhari, A. Iraji, N. Edraki, O. Firuzi, M. Saeedi, M. Mahdavi, T. Akbarzadeh, Synthesis and evaluation of novel arylisoxazoles linked to tacrine moiety: in vitro and in vivo biological activities against Alzheimer's disease, Mol. Divers. 26 (2022) 409–428, https://doi.org/10.1007/s11030-021-10248-w.

[14] D. Bernier, U.K. Wefelscheid, S. Woodward, Properties, preparation and synthetic uses of amine n-oxides. An update, Org. Prep. Proc. Int. 41 (2009) 173–210, https://doi.org/10.1080/00304940902955756.

[15] H. Ibrahim, A. Furiga, E. Najahi, C. Pigasse Hénocq, J.-P. Nallet, C. Roques, A. Aubouy, M. Sauvain, P. Constant, M. Daffé, F. Nepveu, Antibacterial, antifungal and antileishmanial activities of indolone-N-oxide derivatives, J. Antibiot. (Tokyo) 65 (2012) 499–504, https://doi.org/10.1038/ja.2012.60.

[16] J. Balzarini, E. Keyaerts, L. Vijgen, F. Vandermeer, M. Stevens, E. De Clercq, H. Egberink, M. Van Ranst, Pyridine N-oxide derivatives are inhibitory to the human SARS and feline infectious peritonitis coronavirus in cell culture, J. Antimicrob. Chemother. 57 (2006) 472–481, https://doi.org/10.1093/jac/dki481.

[17] A.M. Mfuh, O.V. Larionov, Heterocyclic N-Oxides - an emerging class of therapeutic agents, Curr. Med. Chem. 22 (2015) 2819–2857, https://doi.org/10.2174/0929867322666150619104007.

[18] G.N. Pairas, F. Perperopoulou, P.G. Tsoungas, G. Varvounis, The isoxazole ring and its N -oxide: a privileged core structure in neuropsychiatric therapeutics, ChemMedChem 12 (2017) 408–419, https://doi.org/10.1002/cmdc.201700023.

[19] P. Hlavica, L.A. Damani, B.K. Park, N-oxidation of drugs biochemistry, pharmacology, toxicology, Pharmacogenetics 1 (1991) 165, https://doi.org/10.1097/00008571-199112000-00007.

[20] K. Sharma, Cholinesterase inhibitors as Alzheimer's therapeutics (Review), Mol. Med. Rep. 20 (2019), https://doi.org/10.3892/mmr.2019.10374.

[21] M. Vaz, S. Silvestre, Alzheimer's disease: recent treatment strategies, Eur. J. Pharmacol. 887 (2020) 173554, https://doi.org/10.1016/j.ejphar.2020.173554.

[22] R. Howard, R. McShane, J. Lindesay, C. Ritchie, A. Baldwin, R. Barber, A. Burns, T. Dening, D. Findlay, C. Holmes, A. Hughes, R. Jacoby, R. Jones, R. Jones, I. McKeith, A. Macharouthu, J. O'Brien, P. Passmore, B. Sheehan, E. Juszczak, C. Katona, R. Hills, M. Knapp, C. Ballard, R. Brown, S. Banerjee, C. Onions, M. Griffin, J. Adams, R. Gray, T. Johnson, P. Bentham, P. Phillips, Donepezil and memantine for moderate-to-severe Alzheimer's disease, N. Engl. J. Med. 366 (2012) 893–903, https://doi.org/10.1056/NEJMoa1106668.

[23] C.G. Ballard, Advances in the treatment of Alzheimer's disease: benefits of dual cholinesterase inhibition, Eur. Neurol. 47 (2002) 64–70, https://doi.org/10.1159/000047952.

[24] Y. Bourne, Structural insights into ligand interactions at the acetylcholinesterase peripheral anionic site, EMBO J. 22 (2003) 1–12, https://doi.org/10.1093/emboj/cdg005.

[25] V. Tougu, Acetylcholinesterase: mechanism of catalysis and inhibition, Curr. Med. Chem.-Central Nervous Syst. Agents 1 (2001) 155–170, https://doi.org/10.2174/1568015013358536.

[26] R. Sheng, X. Lin, J. Li, Y. Jiang, Z. Shang, Y. Hu, Design, synthesis, and evaluation of 2-phenoxy-indan-1-one derivatives as acetylcholinesterase inhibitors, Bioorg. Med. Chem. Lett. 15 (2005) 3834–3837, https://doi.org/10.1016/j.bmcl.2005.05.132.

[27] R. Leurs, R.A. Bakker, H. Timmerman, I.J.P. de Esch, The histamine H3 receptor: from gene cloning to H3 receptor drugs, Nat. Rev. Drug Discov. 4 (2005) 107–120, https://doi.org/10.1038/nrd1631.

[28] C. Altug, H. Güneş, A. Nocentini, S.M. Monti, M. Buonanno, C.T. Supuran, Synthesis of isoxazole-containing sulfonamides with potent carbonic anhydrase II and VII inhibitory properties, Bioorg. Med. Chem. 25 (2017) 1456–1464, https://doi.org/10.1016/j.bmc.2017.01.008.

[29] Ö. Kavas, C. Altug, Direct access to 1,4-benzothiazine 4,4-dioxides and 4-oxides via a domino reaction, Tetrahedron 73 (2017) 2656–2661, https://doi.org/10.1016/j.tet.2017.03.056.

[30] B.A. Chalyk, K.V. Hrebeniuk, K.S. Gavrilenko, O.V. Shablykin, O.O. Yanshyna, D. Bash, P.K. Mykhailiuk, O.S. Liashuk, O.O. Grygorenko, Synthesis of Bi- and polyfunctional isoxazoles from amino acid derived halogenoximes and active methylene nitriles, Eur. J. Org. Chem. 2018 (2018) 2753–2761, https://doi.org/10.1002/ejoc.201800311.

[31] C.A. Lipinski, Lead- and drug-like compounds: the rule-of-five revolution, Drug Discov. Today Technol. 1 (2004) 337–341, https://doi.org/10.1016/j.ddtec.2004.11.007.

[32] D. Osmaniye, A.E. Evren, B.N. Sağlık, S. Levent, Y. Özkay, Z.A. Kaplancıklı, Design, synthesis, biological activity, molecular docking, and molecular dynamics of novel benzimidazole derivatives as potential AChE/MAO-B dual inhibitors, Arch. Pharm. (Weinheim) 355 (2022), https://doi.org/10.1002/ardp.202100450.

[33] F. Tok, B. Koçyiğit-Kaymakçıoğlu, B.N. Sağlık, S. Levent, Y. Özkay, Z. A. Kaplancıklı, Synthesis and biological evaluation of new pyrazolone Schiff bases as monoamine oxidase and cholinesterase inhibitors, Bioorg. Chem. 84 (2019) 41–50, https://doi.org/10.1016/j.bioorg.2018.11.016.

[34] B.N. Sağlık, S. Ilgın, Y. Özkay, Synthesis of new donepezil analogues and investigation of their effects on cholinesterase enzymes, Eur. J. Med. Chem. 124 (2016) 1026–1040, https://doi.org/10.1016/j.ejmech.2016.10.042.

[35] G.L. Ellman, K.D. Courtney, V. Andres, R.M. Featherstone, A new and rapid colorimetric determination of acetylcholinesterase activity, Biochem. Pharmacol. 7 (1961) 88–95, https://doi.org/10.1016/0006-2952(61)90145-9.

[36] N. Wang, W. Liu, L. Zhou, W. Liu, X. Liang, X. Liu, Z. Xu, T. Zhong, Q. Wu, X. Jiao, J. Chen, X. Ning, X. Jiang, Q. Zhao, Design, synthesis, and biological evaluation of notopterol derivatives as triple inhibitors of AChE/BACE1/GSK3β for the treatment of Alzheimer's disease, ACS Omega 7 (2022) 32131–32152, https://doi.org/10.1021/acsomega.2c03368.

[37] H. Pourtaher, A. Hasaninejad, A. Iraji, Design, synthesis, in silico and biological evaluations of novel polysubstituted pyrroles as selective acetylcholinesterase inhibitors against Alzheimer's disease, Sci. Rep. 12 (2022) 15236, https://doi.org/10.1038/s41598-022-18224-6.

[38] M.A. Javed, S. Bibi, M.S. Jan, M. Ikram, A. Zaidi, U. Farooq, A. Sadiq, U. Rashid, Diclofenac derivatives as concomitant inhibitors of cholinesterase, monoamine oxidase, cyclooxygenase-2 and 5-lipoxygenase for the treatment of Alzheimer's disease: synthesis, pharmacology, toxicity and docking studies, RSC Adv. 12 (2022) 22503–22517, https://doi.org/10.1039/D2RA04183A.

[39] A.E. Evren, D. Nuha, S. Dawbaa, B.N. Sağlık, L. Yurttaş, Synthesis of novel thiazolyl hydrazone derivatives as potent dual monoamine oxidase-aromatase inhibitors, Eur. J. Med. Chem. 229 (2022) 114097, https://doi.org/10.1016/j.ejmech.2021.114097.

[40] N.Ö. Can, D. Osmaniye, S. Levent, B.N. Sağlık, B. Korkut, Ö. Atlı, Y. Özkay, Z. A. Kaplancıklı, Design, synthesis and biological assessment of new thiazolylhydrazine derivatives as selective and reversible h MAO-A inhibitors, Eur. J. Med. Chem. 144 (2018) 68–81, https://doi.org/10.1016/j.ejmech.2017.12.013.

[41] Ö.D. Can, D. Osmaniye, Ü. Demir Özkay, B.N. Sağlık, S. Levent, S. Ilgın, M. Baysal, Y. Özkay, Z.A. Kaplancıklı, MAO enzymes inhibitory activity of new benzimidazole derivatives including hydrazone and propargyl side chains, Eur. J. Med. Chem. 131 (2017) 92–106, https://doi.org/10.1016/j.ejmech.2017.03.009.

[42] F. Tok, Z. Uğraş, B.N. Sağlık, Y. Özkay, Z.A. Kaplancıklı, B. Koçyiğit-Kaymakçıoğlu, Novel 2,5-disubstituted-1,3,4-oxadiazole derivatives as MAO-B inhibitors: synthesis, biological evaluation and molecular modeling studies, Bioorg. Chem. 112 (2021) 104917, https://doi.org/10.1016/j.bioorg.2021.104917.

[43] M.G. Livingston, H.M. Livingston, Monoamine Oxidase Inhibitors, Drug Saf. 14 (1996) 219–227, https://doi.org/10.2165/00002018-199614040-00002.

[44] J.P.M. Finberg, J.M. Rabey, Inhibitors of MAO-A and MAO-B in Psychiatry and Neurology, Front. Pharmacol. 7 (2016), https://doi.org/10.3389/fphar.2016.00340.

[45] J. Jiménez, S. Doerr, G. Martínez-Rosell, A.S. Rose, G. De Fabritiis, DeepSite: protein-binding site predictor using 3D-convolutional neural networks, Bioinformatics 33 (2017) 3036–3042, https://doi.org/10.1093/bioinformatics/btx350.

[46] C. Binda, J. Wang, L. Pisani, C. Caccia, A. Carotti, P. Salvati, D.E. Edmondson, A. Mattevi, Structures of human monoamine oxidase b complexes with selective noncovalent inhibitors: safinamide and coumarin analogs, J. Med. Chem. 50 (2007) 5848–5852, https://doi.org/10.1021/jm070677y.

[47] J. Cheung, M.J. Rudolph, F. Burshteyn, M.S. Cassidy, E.N. Gary, J. Love, M. C. Franklin, J.J. Height, Structures of human acetylcholinesterase in complex with pharmacologically important ligands, J. Med. Chem. 55 (2012) 10282–10286, https://doi.org/10.1021/jm300871x.

[48] O. Trott, A.J. Olson, AutoDock Vina: improving the speed and accuracy of docking with a new scoring function, efficient optimization, and multithreading, J. Comput. Chem. 31 (2010) 455–461, https://doi.org/10.1002/jcc.21334.

[49] D. Afriza, W.H. Suriyah, S.J.A. Ichwan, In silico analysis of molecular interactions between the anti-apoptotic protein survivin and dentatin, nordentatin, and quercetin, J. Phys. Conf. Ser. 1073 (2018) 032001, https://doi.org/10.1088/1742-6596/1073/3/032001.

[50] E.F. Pettersen, T.D. Goddard, C.C. Huang, G.S. Couch, D.M. Greenblatt, E.C. Meng, T.E. Ferrin, UCSF Chimera—A visualization system for exploratory research and

analysis, J. Comput. Chem. 25 (2004) 1605–1612, https://doi.org/10.1002/jcc.20084.
[51] J.A. Arnott, S.L. Planey, The influence of lipophilicity in drug discovery and design, Expert Opin. Drug Discov. 7 (2012) 863–875, https://doi.org/10.1517/17460441.2012.714363.
[52] S. Forli, R. Huey, M.E. Pique, M.F. Sanner, D.S. Goodsell, A.J. Olson, Computational protein–ligand docking and virtual drug screening with the AutoDock suite, Nat. Protoc. 11 (2016) 905–919, https://doi.org/10.1038/nprot.2016.051.